PI3K pathway inhibition achieves potent antitumor activity in melanoma brain metastases in vitro and in vivo

Niessner, H ; Schmitz, J ; Tabatabai, G ; et al ; Dummer, Reinhard

DOI: https://doi.org/10.1158/1078-0432.CCR-16-0064

PI3K pathway inhibition achieves potent antitumor activity in melanoma brain metastases *in vitro* and *in vivo*.

Heike Niessner[1]*, Jennifer Schmitz[2]*, Ghazaleh Tabatabai[3,4,5,6], Andreas M. Schmid[2], Carsten Calaminus[2], Tobias Sinnberg[1], Benjamin Weide[1], Thomas Eigentler[1], Claus Garbe[1], Birgit Schittek[1], Leticia Quintanilla-Fend[7], Benjamin Bender[8], Marion Mai[9,10], Christian Praetorius[9,10], Stefan Beissert[9], Gabriele Schackert[11], Michael H. Muders[12], Matthias Meinhardt[12], Gustavo Baretton[12], Reinhard Dummer[13], Keith Flaherty[14], Bernd J. Pichler[2], Dagmar Kulms[9,10], Dana Westphal[9,10]* and Friedegund Meier[1,9]*

[1]Department of Dermatology, University Hospital Tübingen, Eberhard Karls University Tübingen Germany

[2]Werner Siemens Imaging Center, Department of Preclinical Imaging and Radiopharmacy, University Hospital Tübingen, Eberhard Karls University Tübingen, Germany

[3]Interdisciplinary Division of Neuro-Oncology, Departments of Vascular Neurology & Neurosurgery, Hertie Institute for Clinical Brain Research, University Hospital Tübingen, Eberhard Karls University Tübingen Germany

[4]Neuro-Oncology Center Tübingen, Comprehensive Cancer Center Tübingen-Stuttgart, Germany

[5]Center for Personalized Medicine, Eberhard Karls University Tübingen, Germany

[6]German Cancer Consortium (DKTK), DKFZ partner site Tübingen, Germany

[7]Department of Pathology, University Hospital Tübingen, Eberhard Karls University Tübingen Germany

[8]Department of Diagnostic and Interventional Neuroradiology, University Hospital Tübingen, Eberhard Karls University Tübingen Germany

[9]Department of Dermatology, Carl Gustav Carus Medical Center, TU Dresden, Germany

[10]Center for Regenerative Therapies Dresden, DFG Research Center and Cluster of Excellence, TU Dresden, Germany

[11]Department of Neurosurgery, Carl Gustav Carus Medical Center, TU Dresden, Germany

[12]Department of Pathology, Carl Gustav Carus Medical Center, TU Dresden, Germany

[13]Department of Dermatology, University Hospital Zürich, Zürich, Switzerland

[14]Massachusetts General Hospital Cancer Center, Harvard Medical School, Boston, USA

*These authors contributed equally to this work

Running title: PI3K inhibition in melanoma brain metastases

Keywords: Melanoma, Brain metastasis, PI3K pathway, AKT, buparlisib

Financial support: The authors of this publication were supported by the German Research Foundation (SFB 773; Friedegund Meier, Heike Niessner, Birgit Schittek and Ghazaleh Tabatabai), Novartis (Friedegund Meier, Heike Niessner), the University of Tübingen (fortuene, Heike Niessner; Demonstratorprojekt, Ghazaleh Tabatabai), the Federal Ministry of Education and Research (FKZ 031A423B; Christian Praetorius, Dagmar Kulms) the German Cancer Aid (110210; Birgit Schittek) and the National Center for Cancer/NCT Program and Infrastructure Grant (Friedegund Meier, Michael H. Muders).

Correspondence

Prof. Dr. med. Friedegund Meier

Dermatoonkologie

Klinik und Poliklinik für Dermatologie

Universitätsklinikum Carl Gustav Carus an der Technischen Universität Dresden

Anstalt des öffentlichen Rechts des Freistaates Sachsen

Fetscherstraße 74

01307 Dresden

Tel. 0351/458-3677

Fax. 0351/458-4338

email: Friedegund.Meier@uniklinikum-dresden.de

http://www.uniklinikum-dresden.de

Disclosure of Potential Conflicts of Interest

The authors declare no conflicts of interest.

Authors' Contributions

Conception and design: Heike Niessner, Jennifer Schmitz, Ghazaleh Tabatabai, Andreas M. Schmid, Carsten Calaminus, Tobias Sinnberg, Benjamin Weide, Claus Garbe, Birgit Schittek, Leticia Quintanilla-Fend, Stefan Beissert, Gabriele Schackert, Michael H. Muders, Matthias Meinhardt, Gustavo Baretton, Keith Flaherty, Bernd J. Pichler, Dagmar Kulms, Dana Westphal, Friedegund Meier

Development of methodology: Heike Niessner, Jennifer Schmitz, Ghazaleh Tabatabai, Andreas M. Schmid, Carsten Calaminus, Tobias Sinnberg, Leticia Quintanilla-Fend, Bernd J. Pichler, Dagmar Kulms, Dana Westphal, Friedegund Meier

Acquisition of data: Heike Niessner, Jennifer Schmitz, Andreas M. Schmid, Tobias Sinnberg, Leticia Quintanilla-Fend, Marion Mai, Dana Westphal

Analysis and interpretation of data: Heike Niessner, Jennifer Schmitz, Ghazaleh Tabatabai, Andreas M. Schmid, Tobias Sinnberg, Benjamin Weide, Claus Garbe, Birgit Schittek, Leticia Quintanilla-Fend, Benjamin Bender, Marion Mai, Christian Praetorius, Stefan Beissert, Gabriele Schackert, Michael H. Muders, Matthias Meinhardt, Gustavo Baretton, Reinhard Dummer, Keith Flaherty, Bernd J. Pichler, Dagmar Kulms, Dana Westphal, Friedegund Meier

Writing and review and/or revision of the manuscript: Heike Niessner, Jennifer Schmitz, Ghazaleh Tabatabai, Andreas M. Schmid, Carsten Calaminus, Tobias Sinnberg, Benjamin Weide, Thomas Eigentler, Claus Garbe, Birgit Schittek, Leticia Quintanilla-Fend, Benjamin Bender, Marion Mai, Christian Praetorius, Stefan Beissert, Gabriele Schackert, Michael H. Muders, Matthias Meinhardt, Gustavo Baretton, Reinhard Dummer, Keith Flaherty, Bernd J. Pichler, Dagmar Kulms, Dana Westphal, Friedegund Meier

Administrative, technical and material support (e.g. providing tumor material, funding support): Heike Niessner, Jennifer Schmitz, Ghazaleh Tabatabai, Andreas M. Schmid, Carsten Calaminus, Thomas Eigentler, Claus Garbe, Leticia Quintanilla-Fend, Marion Mai, Stefan Beissert, Gabriele Schackert, Reinhard Dummer, Bernd J. Pichler, Dagmar Kulms, Dana Westphal, Friedegund Meier

Word count: 4807 (excluding references and figure legends)
Number of figures: 5

Translational relevance

Despite impressive advances with systemic therapies on patients with metastatic melanoma, patients with melanoma brain metastases (MBM) still have a poor overall survival. Identifying and overcoming MBM-specific resistance mechanisms is therefore a major aim in the search for successful treatments. Recent studies have implicated a fundamental role of the PI3K-AKT signaling pathway in survival and growth of melanoma cells in the brain microenvironment. Our studies show that inhibition of the PI3K-AKT pathway leads to growth arrest and induction of apoptosis in brain metastatic melanoma cells *in vitro* and *in vivo*. This provides a strong rationale for targeting this pathway in melanoma patients with brain metastases and will be investigated in a recently initiated clinical trial.

Abstract

Purpose: Great advances have recently been made in treating patients with metastatic melanoma. However, existing therapies are less effective on cerebral than extracerebral metastases. This highlights the potential role of the brain environment on tumor progression and drug resistance and underlines the need for “brain-specific” therapies. We previously showed that the PI3K-AKT survival pathway is hyperactivated in brain but not extracerebral melanoma metastases and that astrocyte-conditioned medium activates AKT in melanoma cells *in vitro*. We therefore tested the PI3K inhibitor buparlisib as an antitumor agent for melanoma brain metastases**.**

Experimental Design and Results: Buparlisib inhibited AKT activity, decreased proliferation and induced apoptosis in metastatic melanoma cell lines and short-term brain melanoma cells, irrespective of their BRAF and NRAS mutation status. Additionally, buparlisib

inhibited hyperactivated AKT and induced apoptosis in melanoma cells that were stimulated with astrocyte-conditioned medium. The growth of tumors induced by injecting human BRAF- and NRAS-mutant metastatic melanoma cells into the brain of mice was significantly inhibited by buparlisib.

Conclusions: These results emphasize the value of targeting the PI3K pathway as a strategy to develop drugs for melanoma brain metastases.

Introduction

Melanoma is one of the most common tumors that metastasizes to the brain. Up to 75% of patients with stage IV melanoma develop brain metastases (1). Brain metastases are associated with significant morbidity and very poor prognosis, showing a median overall survival of 3-6 months (2). Patients with a good performance status, controlled extracerebral metastases, and brain metastases that can be managed by neurosurgery or radiosurgery, have a better prognosis, including long-term survival. The approval of effective systemic drugs has revolutionized the treatment of metastatic melanoma. BRAF inhibitors have demonstrated efficacy in fighting active BRAFV600 mutated melanoma brain metastases. In a phase II trial, the BRAF inhibitor dabrafenib led to an intracranial objective response rate (ORR) of 31-39%, a median progression-free survival (PFS) of 16-17 weeks and a median overall survival (OS) of 31-33 weeks in BRAFV600E-mutated melanoma patients with asymptomatic brain metastases (3). Another phase II study with the BRAF inhibitor vemurafenib in patients with BRAFV600-mutated melanoma and asymptomatic and symptomatic brain metastases displayed an intracranial ORR of 18-20%, a median PFS of 16-18 weeks and a median OS of 28 weeks (4). However, the benefit for these patients is limited by the short response duration and lack of complete

durable responses. The cytotoxic T lymphocyte antigen-4 (CTLA-4) antibody, ipilimumab, has also shown activity in asymptomatic melanoma brain metastases, with an intracranial ORR of 16%, a median PFS of 6 weeks and a median OS of 30 weeks (5). However, the same survival benefit was not evident for patients with symptomatic melanoma brain metastases that are dependent on a high dose of steroids (5). Thus, there is an urgent need for alternative treatments for melanoma patients with brain metastases.

Emerging data on the molecular characteristics of melanoma brain metastases suggest that brain metastases show significant differences compared to extracerebral metastases and primary tumors that may contribute to intracerebral therapy resistance. Whereas treatment with the BRAF inhibitor vemurafenib resulted in partial or complete remission of extracerebral metastases, brain metastases appeared or progressed (6, 7). Immunohistochemical analyses of brain metastases and matched extracerebral metastases revealed the PI3K-AKT signaling pathway but not the RAF-MEK-ERK (MAPK) signaling pathway to be hyperactivated in the brain (6, 7). While levels of ERK, pERK, and AKT appeared to be identical, levels of pAKT were significantly increased in brain metastases. This clinical difference is very significant, because ERK, pERK, AKT, and pAKT expressions were shown to be identical in monolayer cultures derived from melanoma brain and extracerebral metastases. Additionally, melanoma cells cultured in astrocyte-conditioned medium again showed higher AKT activation and invasiveness than when cultured in fibroblast-conditioned medium.

This suggests that brain-derived factors may hyperactivate the AKT survival pathway, promoting invasiveness and drug resistance of melanoma cells in the brain. Thus, inhibition of PI3K-AKT signaling with PI3K inhibitors such as buparlisib may help defeat melanoma brain metastases.

Buparlisib is a potent pan-class I PI3K inhibitor that selectively targets the catalytic isoforms of class IA (p110α, p110β, p110δ) and class IB (p110γ) PI3Ks. Buparlisib inhibits proliferation and induces apoptosis in various tumor cell lines (8, 9). Furthermore, it inhibits the growth of human tumors in xenograft mouse models in a well-tolerated manner and very efficiently penetrates the blood-brain barrier (8-10). Buparlisib reduced glioblastoma tumor spread in orthotopic xenograft models (11). A phase I clinical trial using buparlisib on a variety of solid tumors showed good disease control and tolerable toxicity (12). Additionally, a clear clinical benefit was demonstrated in breast cancer patients treated with buparlisib alone (13). Recently, phase II and phase III clinical trials have been extended to lung cancer, head and neck cancer and glioblastoma. Several studies suggest that the antitumor effects are enhanced when buparlisib is combined with other anticancer agents. For instance, combination of buparlisib with fulvestrant in endocrine-resistant HR+/HER2- breast cancer significantly improved PFS, ORR and CBR (clinical benefit rate), particularly in patients with mutated PIK3CA (phosphatidylinositol-4,5-bisphosphate 3-kinase catalytic subunit alpha) (14).

Taken together, the favorable properties of the PI3K inhibitor buparlisib in terms of potency, selectivity, brain penetrance, and the reported clinical benefit in other cancers make it a good candidate for treating patients with melanoma brain metastases. We therefore wanted to investigate the antitumor activity of buparlisib in melanoma brain metastases *in vitro* and *in vivo*.

Materials and Methods

Isolation and culture of human cells

We used human metastatic melanoma cell lines, which were BRAF-mutant (WM3734, 451Lu, A375, SKMel19), NRAS-mutant (SKMel147, WM1346, WM1366, MelJuso) or BRAF/NRAS wt (ZueMel1H). The cell lines were kindly provided by M. Herlyn, K. Smalley and R. Dummer or purchased from the American Type Culture Collection. In addition, we used the patient derived brain tumor cell lines M10 (BRAF-mutant), TueMel32H (NRAS-mutant), ZueMel2H, TueMel20H and TueMel41H, respectively. The cells were cultured in RPMI 1640 medium supplemented with 10% FBS and 1% penicillin/streptomycin. Melanoma cell lines, cells isolated from excised brain or extracerebral melanoma metastases, and fibroblasts were isolated and cultured as described previously (15). All patients provided written consent. The use of human tissues in this study was approved by the medical ethical committee of the Universities of Dresden, Zürich and Tübingen and performed in accordance with the Declaration of Helsinki Principles.

Signaling pathway inhibitors and treatments

For blockade of the RAF-MEK-ERK pathway, the BRAF inhibitor encorafenib (Novartis) and the MEK inhibitor binimetinib (Novartis) were employed. For inhibition of the PI3K-AKT pathway, the PI3K inhibitor buparlisib (Novartis) was used. The inhibitors were added at concentrations ranging from 0.3 to 10 μM to the culture medium of cells with 50-70% confluency. Controls were incubated with dimethylsulfoxide (DMSO) alone.

Western blot analyses

After 1-24 h incubation with the inhibitors, the cells were lysed directly in the dish for 30 min on ice with buffer containing 10 mM Tris pH 7.5, 0.5% Triton X-100, 5 mM EDTA, 0.1

μM phenylmethanesulphonylfluoride, 10 μM Pepstatin A, 10 μM Leupeptin, 25 μM aprotinin, 20 mM NaF, 1 mM pyrophosphate, 1 mM orthovanadate. Lysates were cleared by centrifugation at 13,000 *g* for 30 min and 15– 60 μg protein was subjected to SDS-PAGE and transferred to polyvinylidene difluoride (PVDF) membranes. Proteins were detected with Cell Signaling primary antibodies (AKT #9272, pAKTSer473 #4060, ERK #9102, pERKThr202/Tyr204 #4376 and β-Actin #4970) and HRP-conjugated secondary antibodies (Amersham), and membranes were exposed to X-ray film (Eastman Kodak). All images were scanned and cropped in the Adobe Photoshop editing software.

Growth assay (MUH assay)

Cells seeded in quadruplicates in 96-well plates were treated with the various inhibitors for 72 h, washed twice with PBS and then incubated with 100 μl of a solution containing 100 μg/ml 4-methylumbelliferyl-heptanoate (MUH) in PBS for 1 h at 37°C. The absolute fluorescence intensity at λ_{ex} of 355 nm and λ_{em} of 460 nm was measured using a Fluoroskan II device (Labsystems). The intensity of fluorescence corresponds to the number of viable cells.

Cell-cycle analysis

Cells seeded in triplicates in 6-well plates were treated with buparlisib for 72 h. Floating and adherent cells were harvested, washed with PBS and fixed in ice-cold 70% ethanol overnight. After washing twice with cold PBS, cells were stained with 500 μl propidium iodide solution (propidium iodide 40 μg/ml and RNase 100 μg/ml in PBS) for 20 min at 4°C. The cell cycle was analyzed using flow cytometry and FACSDiva software (BD Biosciences).

Immunohistochemistry

For immunohistochemical analysis, human tumor tissue was fixed in 4% formalin, embedded in paraffin and stained with H&E, HMB45 (Dako #M0634) or pAKTSer473 (CellSignaling #4060). Bound antibodies were detected using UltraView Universal Alkaline Phosphatase Red Detection kits from Ventana (Tucson).

Immunofluorescent labelling

Human tumor tissue embedded in paraffin was prepared as described above. Sections were blocked for 5 min with Ultra V Block solution (Thermo Scientific) and then incubated overnight with antibodies against cleaved PARP (CellSignaling #5625) and MIB1 (Ki67, DAKO #M7240). Sections were washed with PBS and incubated for 1 h with a Cy3-coupled donkey-anti-mouse secondary antibody or a Cy5-coupled donkey-anti-rabbit antibody (Dianova, Hamburg, Germany). Nuclei were detected with YOPRO (Molecular Probes, Leiden Netherlands). Samples were analyzed using a Leica TCS SP confocal microscope (Leica, Wetzlar, Germany).

***In vivo* mouse model**

Stereotactic inoculation of melanoma cells into the brain of nude mice

In a stereotactic surgical procedure 150,000 human melanoma cells (WM3734 or SKMel147) were injected into the right striatum of 8-week-old female CD1nu/nu mice (Charles River Laboratories). All animals were housed under standardized environmental conditions (20 ± 1°C room temperature, 50 ± 10% relative humidity, and 12 h light-dark phases) with free access to food and water *ad libitum*. To achieve sufficient analgesia the mice were injected i.p. with Meditomidin/Midazolam/Fentanyl (0.5/5/0.05 mg/kg body weight). The anesthetized animals were positioned in the stereotactic apparatus by fixing

the head in the ear bars. After opening the skin and the skull, the cells were injected with a Hamilton syringe (150,000 cells in 3 µl) using a stereotactic holder to insert the syringe into the mouse brains. Afterwards the wound was sutured and the mice were given carprofen (5 mg/kg body weight, twice daily, for 2-3 days s.c.) postoperatively.

All experiments were performed according to the animal use and care protocol (§8 21.06.2012) of the German Animal Protection Law and approved by the Regierungspräsidium Tübingen.

Evaluation of the tumor volume

The tumor volume was evaluated by MRI (BRAF-mutant tumors: Icon (1T-MRI; Multi slice multi echo (MSME) Sequence, repetition time (TR) = 2931 ms, echo time (TE) = 60 ms, 188 x 88 matrix, 22 x 45 mm field of view, slice thickness (ST) = 0.75 mm) and NRAS-mutant tumors: ClinScan (7T-MRI; Turbo spin echo (TSE) Sequence, TR = 3000 ms, TE = 205 ms, 256 x 161 matrix, 35 x 57 mm field of view, ST = 0.22 mm from Bruker BioSpin GmbH) and analyzed using the software Inveon Research Workplace (Siemens Preclinical Solutions). The first measurement was performed 15-16 days post inoculation. After the start of the therapy at day 20 post inoculation the animals were monitored twice weekly. All mice were sacrificed at the onset of neurological symptoms, at 20% loss in weight or at the latest 34 days after inoculation. The brains were excised and fixed in formalin for immunohistochemical analysis.

For mean value analyses, only the mice with a tumor volume ≥ 3 mm^3 when treatment was commenced were included. For all tumors the absolute tumor volume (Fig. 5) as well as the relative tumor volume (Fig. S6), normalized by the volume at treatment induction, was analyzed. Exponential fitting was applied on the tumor growth curves of the absolute tumor

volume. Kaplan-Meier-plots were generated on the basis of animals reaching the endpoint criteria of 20% loss in weight.

Treatment of animals

Buparlisib was administered daily (30 mg/kg body weight) on 14 consecutive days (8, 9), starting 20 days after the tumor inoculation, when the tumors were clearly visible in the MRI scans.

Statistical analysis

Statistical analysis was performed with GraphPad Prism version 5.01 (GraphPad Prism Software Inc.). The differences between the two groups were compared using the nonparametric Mann-Whitney Test (95% CI). P-values <0.05 were considered statistically significant. N-values represent the number of independent experiments unless stated otherwise.

Statistical analysis of the *in vivo* MRI growth data was performed using JMP® Statistical Discovery version 11.0.0. The difference between the treated and the sham groups for multiple time points was analyzed using a Tukey-HSD posthoc test.

Results

The PI3K inhibitor buparlisib inhibits AKT phosphorylation and cell growth in metastatic melanoma cell lines with different mutation signatures

We and others previously showed that the PI3K-AKT pathway is hyperactivated in melanoma brain metastases. Moreover, melanoma cells stimulated with astrocyte-conditioned medium showed increased AKT activation and invasiveness. Based on these

results, we investigated whether the PI3K inhibitor buparlisib could be implemented as an antitumor agent for melanoma brain metastases.

To verify that buparlisib inhibits the PI3K-AKT pathway, the phosphorylation status of AKT was investigated in three metastatic melanoma cell lines carrying different mutation signatures (BRAFV600E: WM3734; NRASQ61R: SKMel147; BRAF/NRASwt: ZueMel1H). Buparlisib effectively inhibited the phosphorylation of AKT in a dose-dependent manner in all of the cell lines independent of the mutation status (Fig. 1A). Consistenly, buparlisib inhibited growth of all three cell lines by 60-70%, as measured by the fluorimetric 4-methylumbelliferyl heptanoate (MUH) assay (Fig. 1B).

Similar results were obtained with six other BRAF- or NRAS-mutated metastatic melanoma cell lines (Supplementary Fig. S1 and S2), confirming that buparlisib effectively inhibits AKT phosphorylation and proliferation of a variety of melanoma cell lines *in vitro*.

Growth inhibition is enhanced when the PI3K inhibitor buparlisib is combined with a MEK inhibitor

In order to test whether the PI3K inhibitor buparlisib can augment the effect of specific MEK and BRAF inhibitors, the three different metastatic melanoma cell lines were tested for growth inhibition after treatment with each of these inhibitors alone or in combination.

The MEK inhibitor binimetinib alone inhibited proliferation by 50-60% in the BRAF- and NRAS-mutated, and by 20% in the BRAF/NRAS wildtype metastatic melanoma cells, while co-treatment with buparlisib yielded significantly higher growth-inhibition (80%) (Supplementary Fig. S3A).

Since treatment of BRAFV600E metastatic melanoma cells with increasing concentrations of the BRAF inhibitor encorafenib alone already inhibited cell growth by 80%, co-treatment with buparlisib did not yield additional improvement (Supplementary Fig. S3B).

Furthermore, AKT phosphorylation was inhibited by buparlisib, with or without encorafenib or binimetinib, starting within 1 h after stimulation (Supplementary Fig. S3C). Inhibition of AKT phosphorylation was still effective after 24 h. As expected, pERK levels were inhibited by binimetinib and encorafenib, but remained unaffected by buparlisib at 1 h and 24 h after treatment.

In summary, combining MEK and PI3K inhibitors inhibits growth more effectively than specific MEK inhibitors alone, regardless of the mutation status of the target cell. In all cases growth inhibition coincided with siginificant reduction of pAKT as well as pERK levels. In contrast, the PI3K inhibitor did not augment the efficacy of the BRAF inhibitor in the BRAF-mutated cell line.

The PI3K inhibitor buparlisib induces apoptosis in metastatic melanoma cell lines

To investigate whether growth inhibition induced by buparlisib also coincides with induction of cell death, cell cycle analysis was performed for all three mutation-specific melanoma cell lines. Buparlisib treatment caused a cell-cycle arrest in the G2/M phase in the BRAF-mutated cell line, and additionally a 20-50% increase of cells in the sub-G1 phase (apoptotic cells) in all cell lines tested (Fig. 2 A and B). Similar results were obtained with six other BRAF- and NRAS-mutant metastatic melanoma cell lines, confirming the ability of buparlisib to drive a variety of melanoma cell lines into apoptotic cell death (Supplementary Fig. S1C and S2C).

The PI3K inhibitor buparlisib inhibits proliferation and induces apoptosis in short-term brain melanoma cells

To add more *in vivo* relevance to the growth inhibitory and cell death inducing effects of buparlisib two melanoma cell lines (BRAF- und NRAS-mutated) directly isolated from

excised brain metastases of patients were investigated. In accordance with our previous observations, activated AKT was significantly decreased after buparlisib treatment as shown by Western Blot analysis (Fig. 3A). Buparlisib also inhibited growth by up to 70% in these as well as three other short-term brain melanoma cell lines (Fig. 3B and Supplementary Fig. S4). Furthermore, buparlisib caused G2/M arrest and a 15% increase in apoptosis in the BRAF-mutated cell line, and a 40% increase in apoptosis in the NRAS-mutated cell line (Fig. 3C and 3D).

In contrast, non-tumor-derived cells of human skin such as fibroblasts stayed largely resistant to buparlisib, with growth being inhibited by only 40% at the highest buparlisib concentration and no increased apoptosis (Supplementary Fig. S5A). Together, these findings strongly imply that buparlisib selectively acts on tumor cells.

The PI3K inhibitor buparlisib inhibits AKT activation and induces apoptosis in metastatic melanoma cell lines stimulated with astrocyte-conditioned medium

In order to evaluate buparlisib for the treatment of brain metastases, we mimicked the brain environment *in vitro* by culturing WM3734 brain-metastatic melanoma cells in astrocyte-conditioned medium. As seen before, astrocyte- but not fibroblast-conditioned medium increased the pAKT levels in WM3734 cells, which were completely inhibited by addition of 1 μM buparlisib (Fig. 4A). Moreover, the PI3K inhibitor buparlisib induced apoptosis in approximately 20% of melanoma cells (Fig. 4B and 4C), indicating that buparlisib can successfully combat the changes being induced by the brain microenvironment.

The PI3K inhibitor buparlisib inhibits growth of BRAF- and NRAS-mutant melanoma in the brain of nude mice

The encouraging results of buparlisib antitumor activity on melanoma cells placed in an artificial brain microenvironment, prompted us to assess its effects on intracranial tumor growth using an *in vivo* mouse model of orthotopically transplanted human BRAF-mutant and NRAS-mutant melanoma brain metastases.

Excitingly, mice treated with the PI3K inhibitor buparlisib showed no further tumor growth, while mice treated only with the vehicle developed rapidly growing tumors in the brain, in both, the BRAF- and the NRAS-mutated tumors (Fig. 5A). Significant differences in relative tumor volumes (Supplementary Fig. S6A) as well as in absolute tumor volumes (Fig. 5B) between the buparlisib and sham treated mice were observed 7 days after treatment onset (day 27 post inoculation) for the BRAF-mutant cells and 6 days after treatment induction (day 26 post inoculation) for the NRAS-mutant cells. For both cell lines exponential fitting was applied to the growth curves of all tumors, verifying the inhibition of the exponential growth pattern of all tumors in the buparlisib treated animals against the sham treated controls (Supplementary Fig. S6B). After 34 days a Kaplan-Meier-plot showed moderate survival for both the sham and the treatment group in the BRAF-mutant tumor mice but dramatically improved survival in the treatment group for the NRAS-mutant tumors (Fig. 5C).

The 7T TSE MRI data of the NRAS-mutated tumors allowed us to identify T2 hyperintense regions indicative of hemorrhages and cysts as well as peritumoral edema (Supplementary Fig. S6C). Peritumoral edema was mild and not seen in all animals. Interestingly, there was a remarkable increase of T2 hyperintense regions in the therapy group, with multifocal intratumoral areas of liquid indicative of hemorrhages or cysts. In the sham group most tumors appeared relatively homogeneous and with distinctively fewer T2 hyperintense areas.

H&E staining of untreated and treated BRAF- and NRAS-mutant tumors confirmed what was seen in the MRI (Supplementary Fig. S7A). Intratumoral bleeding was seen in both treatment groups, but was considerably higher in the buparlisib-treated group (Supplementary Fig. S7B). Necrosis was detected in all untreated NRAS-mutant tumors, highlighting the aggressiveness of the NRAS-mutant tumors (Supplementary Fig. S7C). However, there were also areas of tumor regression, in which the tumor shrank and was replaced by water-filled pseudo-cysts (Supplementary Fig. S7D). Buparlisib caused a substantial increase of these pseudo-cysts in the treated NRAS-mutant tumors, with M12 exhibiting up to 70% of tumor regression.

The effectiveness of buparlisib could also be visualized in immunohistochemical stainings for pAKT and immunofluorescence stainings for Ki67 (proliferation marker) and cleaved PARP (apoptosis marker) (Supplementary Fig. S8). Although buparlisib could not induce sufficient apoptosis to achieve clearance of the tumors (Supplementary Fig. S8A and C), it almost completely inhibited proliferation and tumor growth (Supplementary Fig. S8B and D). As expected, AKT activation was completely prevented by buparlisib (Supplementary Fig. 8E).

In summary, the PI3K inhibitor buparlisib inhibited growth of BRAF-mutant, and even more effectively of NRAS-mutant melanoma cells in the brain of mice, providing evidence for its potent antitumor activity on melanoma brain metastases *in vivo*.

DISCUSSION

Recently, impressive novel treatment strategies have been developed for patients with metastatic melanoma, particularly through inhibiting the RAF-MEK-ERK signaling pathway and by immunotherapy. Although these systemic therapies have been remarkably

successful in fighting metastatic melanoma, patients frequently develop brain metastases during these therapies. So far, little is known about how melanoma brain metastases evade existing therapies. Investigating matched samples from melanoma patients with both cerebral and extracerebral metastases, the PI3K-AKT signaling pathway was found to be upregulated in cerebral compared to extracerebral metastases (6, 16). This prompted us to investigate the antitumor activity of the PI3K inhibitor buparlisib in melanoma brain metastases *in vitro* and *in vivo*.

We show here that buparlisib prevented AKT activation and cell growth of a variety of metastatic melanoma cell lines *in vitro*. In addition, it caused an arrest in the G2/M phase and induced apoptosis to varying degrees in these cell lines.

Our *in vivo* experiments demonstrated robust inhibition of AKT activation as well as proliferation of human melanoma cells implanted into the brain of mice, indicating that buparlisib crosses the blood-brain barrier, as suggested by earlier xenograft experiments (8, 9). The inhibitory effect of buparlisib prevailed irrespective of the BRAF or NRAS mutation status. In particular in mice with NRAS-mutated brain tumors treatment with buparlisib provided a survival benefit compared to sham treatment. Although the tumors were smaller in the BRAF-mutated group, mice of both, the sham and the treatment group showed rapid weight loss, reaching the endpoint of 20% loss in weight faster than the NRAS-mutated group. Evaluation of the tumor sections suggested a fundamental difference between the NRAS- and BRAF-mutated tumors. Although the NRAS-mutated tumors seemed to be more aggressive, the inhibitory effect of buparlisib was much more prominent in these tumors compared to BRAF-mutated tumors. As RAS but not RAF can signal through the PI3K-AKT pathway, NRAS-mutated tumors are probably more sensitive to PI3K pathway inhibition than BRAF-mutated tumors. However, more extensive experiments would be needed to further investigate this prediction.

In our *in vitro* experiments, the combination of the PI3K inhibitor buparlisib with a MEK or BRAF inhibitor led to robust inhibition of AKT and ERK activation. Furthermore, combining the PI3K inhibitor buparlisib with the MEK inhibitor binimetinib inhibited the growth of the melanoma cell lines significantly better than the PI3K or MEK inhibitor alone, irrespective of the mutation status. These data are in line with recent *in vivo* studies. In a BRAF inhibitor resistant patient-derived xenograft model, tumor growth was significantly better controlled by buparlisib in combination with encorafenib plus binimetinib compared to buparlisib or encorafenib plus binimetinib alone (17). Similar results were obtained when the PI3K inhibitor buparlisib was combined with the ERK inhibitor VX-11e (17).

In our BRAF-mutated brain metastatic melanoma cells the PI3K inhibitor buparlisib did not enhance the potent growth inhibition by the BRAF inhibitor encorafenib. However, in a pilot study, combinations of buparlisib and encorafenib improved the survival of mice with intracranial BRAF-mutated tumors compared to encorafenib alone (16). Accordingly, similar findings were obtained by using another BRAF inhibitor (PLX4720) and pan-PI3K inhibitor (PX-866) (18).

These data suggest that combining the PI3K inhibitor buparlisib with a BRAF/MEK inhibitor may prolong response duration and survival in melanoma patients with BRAF-mutated brain metastases. However, a preliminary study of eight cases in which buparlisib was combined with the BRAF inhibitor vemurafenib was not as successful, as half the patients developed dose limiting toxicities such as myalgia, DRESS syndrome and febrile neutropenia, and only one of the eight patients showed a mixed response to the treatment (19). Given that in breast cancer clinical trials combination treatment with buparlisib and the estrogen-receptor antagonist fulvestrant significantly improved the overall survival in the absence of severe side effects (14), further clinical trials of buparlisib or other PI3K

inhibitors in combination with RAF/MEK inhibitors will be required to determine the actual clinical benefit.

Since buparlisib inhibits class I PI3 kinases with similar potency, the present data do not resolve which PI3K isoforms within the PI3K-AKT signaling cascade are being activated by the brain microenvironment. Isoform selective inhibitors are currently being clinically investigated, and could offer an alternative strategy if a pan-PI3K inhibitor such as buparlisib is not tolerated in combination with MAP kinase pathway inhibitors.

Our data on buparlisib inhibiting AKT activation and decreasing growth of human melanoma cells in the brain of mice highlights the importance of the PI3K-AKT pathway in the survival and growth of brain metastatic melanoma cells and is nicely in line with previous reports. Multidimensional molecular profiling of matched cerebral and extracerebral melanoma metastases found no differences in hotspot mutations, copy-number variations, mRNA and protein expression, but detected increased expression of several activation-specific protein markers of the PI3K-AKT pathway in brain metastases (16). Furthermore, in a retrospective analysis, complete loss of the phosphatase PTEN, which inhibits PI3K, correlated with more rapid brain metastasis formation and decreased overall survival in stage IIIB/C melanoma patients with BRAFV600 mutations (20). A recent study suggested a functional crosstalk between PI3K-AKT signaling and PLEKHA5 to exist in melanoma brain metastases (21). PLEKHA5 was overexpressed in cerebrotropic A375 melanoma cells, and its knockdown stopped the cells from proliferating and migrating across the blood-brain barrier *in vitro*. PLEKHA5 possesses a pleckstrin homology domain that facilitates recruitment to the plasma membrane and binding to phosphoinositides such as PIP3 (22). As PIP3 is generated by the PI3-kinase, a PI3K inhibitor such as buparlisib might inhibit PLEKHA5 membrane association and its function.

When staining the untreated versus treated NRAS- and BRAF-mutated tumors for PLEKHA5, we found that PLEKHA5 was significantly decreased in the buparlisib-treated tumors (Supplementary Fig. S9). One may speculate that after loss of its membrane association, PLEKHA5 is targeted for proteasomal degradation. As PLEKHA5 expression correlates with the early onset of melanoma brain metastases (21), PI3K inhibition may be a new strategy to affect melanoma brain metastasis formation via targeting PLEKHA5.

We observed that mimicking the brain environment *in vitro* by stimulating metastatic melanoma cells with astrocyte-conditioned medium increased the pAKT levels. Buparlisib completely prevented this increase and induced apoptosis in these cells. These results illustrate how the brain microenvironment activates the PI3K-AKT pathway, potentially allowing brain metastases to resist therapy. Several studies have demonstrated interactions between astrocytes and tumor cells including melanoma cells. The interaction with astrocytes upregulates multiple genes in melanoma cells, including several survival genes that increase their resistance to cytotoxic drugs (23). It has been demonstrated recently that astrocytes epigenetically repress expression of the negative regulator of PI3K signaling, PTEN, in metastatic tumor cells (24). Another experimental study showed that brain-metastatic melanoma cells acquire neuron-like characteristics (25), which may intensify their interactions with normal brain cells and promote survival and growth (25). This brain-specific signature overlaps with previous data showing significant transcript differences between melanoma cells harvested from the brain compared to other metastatic sites (26). Moreover, interactions between astrocytes and melanoma cells seem to be reciprocal, as melanoma cells can reprogram astrocytes to express IL-23 (27). This inflammatory cytokine in turn causes the melanoma cells to secrete the matrix metalloproteinase MMP2, thereby enhancing their invasiveness (27).

In conclusion, our data provide evidence that hyperactivation of the PI3K-AKT pathway is a prominent feature of melanoma brain metastases. Even though the molecular mechanisms underlying PI3K-AKT hyperactivation remain to be determined, our data provide a strong rationale for targeting this pathway in melanoma patients with brain metastases. Combinations of PI3K inhibitors with BRAF or MEK inhibitors may significantly increase antitumor activity and prolong survival. A phase II trial of buparlisib in patients with stage IV melanoma and brain metastases has been initiated (NCT02452294). The results will further increase our knowledge about the potential of buparlisib for treating melanoma brain metastases.

Acknowledgements

The authors would like to thank Funda Cay, Laura Kübler, Sandro Aidone and Julia Lagler for excellent technical assistance. We thank Michelle Meredyth-Stewart for critical reading of the manuscript.

References

1. Eisele SC, Gill CM, Shankar GM, Brastianos PK. PLEKHA5: A Key to Unlock the Blood-Brain Barrier? Clinical cancer research : an official journal of the American Association for Cancer Research. 2015;21:1978-80.
2. Davies MA, Liu P, McIntyre S, Kim KB, Papadopoulos N, Hwu WJ, et al. Prognostic factors for survival in melanoma patients with brain metastases. Cancer. 2011;117:1687-96.

3. Long GV, Trefzer U, Davies MA, Kefford RF, Ascierto PA, Chapman PB, et al. Dabrafenib in patients with Val600Glu or Val600Lys BRAF-mutant melanoma metastatic to the brain (BREAK-MB): a multicentre, open-label, phase 2 trial. The Lancet Oncology. 2012;13:1087-95.
4. Kefford RF, Maio M, Arance A, Nathan P, Blank C, Avril MF, et al. Vemurafenib in metastatic melanoma patients with brain metastases: an open-label, single-arm, phase 2, multicenter study. Society of Melanoma Research. Philadelphia: Pigment Cell Melanoma Research; 2013. p. 932-1019.
5. Margolin K, Ernstoff MS, Hamid O, Lawrence D, McDermott D, Puzanov I, et al. Ipilimumab in patients with melanoma and brain metastases: an open-label, phase 2 trial. The Lancet Oncology. 2012;13:459-65.
6. Niessner H, Forschner A, Klumpp B, Honegger JB, Witte M, Bornemann A, et al. Targeting hyperactivation of the AKT survival pathway to overcome therapy resistance of melanoma brain metastases. Cancer medicine. 2013;2:76-85.
7. Peuvrel L, Saint-Jean M, Quereux G, Brocard A, Khammari A, Knol AC, et al. Incidence and characteristics of melanoma brain metastases developing during treatment with vemurafenib. Journal of neuro-oncology. 2014;120:147-54.
8. Koul D, Fu J, Shen R, LaFortune TA, Wang S, Tiao N, et al. Antitumor activity of NVP-BKM120--a selective pan class I PI3 kinase inhibitor showed differential forms of cell death based on p53 status of glioma cells. Clinical cancer research : an official journal of the American Association for Cancer Research. 2012;18:184-95.
9. Maira SM, Pecchi S, Huang A, Burger M, Knapp M, Sterker D, et al. Identification and characterization of NVP-BKM120, an orally available pan-class I PI3-kinase inhibitor. Molecular cancer therapeutics. 2012;11:317-28.

10. Wen PY, Lee EQ, Reardon DA, Ligon KL, Alfred Yung WK. Current clinical development of PI3K pathway inhibitors in glioblastoma. Neuro-oncology. 2012;14:819-29.
11. Speranza MC, Nowicki MO, Behera P, Cho CF, Chiocca EA, Lawler SE. BKM-120 (Buparlisib): A Phosphatidyl-Inositol-3 Kinase Inhibitor with Anti-Invasive Properties in Glioblastoma. Scientific reports. 2016;6:20189.
12. Bendell JC, Rodon J, Burris HA, de Jonge M, Verweij J, Birle D, et al. Phase I, dose-escalation study of BKM120, an oral pan-Class I PI3K inhibitor, in patients with advanced solid tumors. Journal of clinical oncology : official journal of the American Society of Clinical Oncology. 2012;30:282-90.
13. Ando Y, Inada-Inoue M, Mitsuma A, Yoshino T, Ohtsu A, Suenaga N, et al. Phase I dose-escalation study of buparlisib (BKM120), an oral pan-class I PI3K inhibitor, in Japanese patients with advanced solid tumors. Cancer science. 2014;105:347-53.
14. Baselga J, Im S-A, Iwata H, Clemons M, Ito Y, Awada A, et al. PIK3CA status in circulating tumor DNA (ctDNA) predicts efficacy of buparlisib (BUP) plus fulvestrant (FULV) in postmenopausal women with endocrine-resistant HR+/HER2- advanced breast cancer (BC): First results from the randomized, phase III BELLE-2 trial. San Antonio Breast Cancer Symposium. San Antonio: SABCS online Symposium proceedings (Supplement to Cancer Research); 2015.
15. Meier F, Nesbit M, Hsu MY, Martin B, Van Belle P, Elder DE, et al. Human melanoma progression in skin reconstructs : biological significance of bFGF. The American journal of pathology. 2000;156:193-200.
16. Chen G, Chakravarti N, Aardalen K, Lazar AJ, Tetzlaff MT, Wubbenhorst B, et al. Molecular profiling of patient-matched brain and extracranial melanoma metastases

implicates the PI3K pathway as a therapeutic target. Clinical cancer research : an official journal of the American Association for Cancer Research. 2014;20:5537-46.

17. Krepler C, Xiao M, Sproesser K, Brafford PA, Shannan B, Beqiri M, et al. Personalized Preclinical Trials in BRAF Inhibitor-Resistant Patient-Derived Xenograft Models Identify Second-Line Combination Therapies. Clinical cancer research : an official journal of the American Association for Cancer Research. 2016;22:1592-602.
18. Shannan B, Chen Q, Watters A, Perego M, Krepler C, Thombre R, et al. Enhancing the evaluation of PI3K inhibitors through 3D melanoma models. Pigment cell & melanoma research. 2016.
19. Algazi AP, Posch C, Ortiz-Urda S, Cockerill A, Munster PN, Daud A. A phase I trial of BKM120 combined with vemurafenib in BRAFV600E/K mutant advanced melanoma. 50th Annual Meeting of American Society Of Clinical Oncology Chicago: J Clin Oncol; 2014.
20. Bucheit AD, Chen G, Siroy A, Tetzlaff M, Broaddus R, Milton D, et al. Complete loss of PTEN protein expression correlates with shorter time to brain metastasis and survival in stage IIIB/C melanoma patients with BRAFV600 mutations. Clinical cancer research : an official journal of the American Association for Cancer Research. 2014;20:5527-36.
21. Jilaveanu LB, Parisi F, Barr ML, Zito CR, Cruz-Munoz W, Kerbel RS, et al. PLEKHA5 as a Biomarker and Potential Mediator of Melanoma Brain Metastasis. Clinical cancer research : an official journal of the American Association for Cancer Research. 2015;21:2138-47.
22. Zou Y, Zhong W. A likely role for a novel PH-domain containing protein, PEPP2, in connecting membrane and cytoskeleton. Biocell : official journal of the Sociedades Latinoamericanas de Microscopia Electronica et al. 2012;36:127-32.

23. Kim SJ, Kim JS, Park ES, Lee JS, Lin Q, Langley RR, et al. Astrocytes upregulate survival genes in tumor cells and induce protection from chemotherapy. Neoplasia (New York, NY). 2011;13:286-98.
24. Zhang L, Zhang S, Yao J, Lowery FJ, Zhang Q, Huang WC, et al. Microenvironment-induced PTEN loss by exosomal microRNA primes brain metastasis outgrowth. Nature. 2015;527:100-4.
25. Nygaard V, Prasmickaite L, Vasiliauskaite K, Clancy T, Hovig E. Melanoma brain colonization involves the emergence of a brain-adaptive phenotype. Oncoscience. 2014;1:82-94.
26. Park ES, Kim SJ, Kim SW, Yoon SL, Leem SH, Kim SB, et al. Cross-species hybridization of microarrays for studying tumor transcriptome of brain metastasis. Proceedings of the National Academy of Sciences of the United States of America. 2011;108:17456-61.
27. Klein A, Schwartz H, Sagi-Assif O, Meshel T, Izraely S, Ben Menachem S, et al. Astrocytes facilitate melanoma brain metastasis via secretion of IL-23. The Journal of pathology. 2015;236:116-27.

Figure legends

Figure 1: The PI3K inhibitor buparlisib inhibits AKT phosphorylation and cell growth in metastatic melanoma cell lines

(A) WM3734 (BRAF-mutant), SKMel147 (NRAS-mutant) and ZueMel1H (BRAF/NRASwt) metastatic melanoma cell lines were treated with increasing concentrations of the PI3K inhibitor buparlisib for 6 h and were subjected to Western Blot analysis of AKT and pAKT.

β-Actin was detected as a loading control. Western Blot is representative of three independent experiments. Western Blots of 8 other BRAF- or NRAS-mutant cell lines are shown in Fig. 3, S1 and S2. (B) Metastatic melanoma cells were treated with buparlisib for 72 h and subjected to a growth inhibition assay (MUH assay). The percentage of growth inhibition was compared to DMSO-treated controls. Error bars represent SD of three independent experiments. Growth inhibition assays of 11 other BRAF- or NRAS-mutant cell lines are shown in Fig. 3, S1, S2 and S4.

Figure 2: The PI3K inhibitor buparlisib induces apoptosis in metastatic melanoma cell lines

WM3734 (BRAF-mutant), SKMel147 (NRAS-mutant) and ZueMel1H (BRAF/NRASwt) metastatic melanoma cell lines were treated with increasing concentrations of the PI3K inhibitor buparlisib for 72 h and subjected to cell cycle analysis by flow cytometry. Histograms in (A) are representative of triplicate experiments. The percentage of cells in <G1, G1, S and G2/M phase was quantified and displayed in a stacked bar graph (B). Error bars represent SD of triplicate experiments. Cell-cycle analysis of 8 other BRAF- or NRAS-mutant cell lines is shown in Fig. 3, S1 and S2.

Figure 3: The PI3K inhibitor buparlisib inhibits AKT phosphorylation and cell growth and induces cell cycle arrest and apoptosis in short-term brain melanoma cell lines

(A) Brain derived melanoma cells were treated with increasing concentrations of the PI3K inhibitor buparlisib for 6-12 h and were subjected to Western Blot analysis of AKT and pAKT. β-Actin was detected as a loading control. Western Blot is representative of three independent experiments. (B) Brain melanoma cells were treated with buparlisib for 72 h and then subjected to a growth inhibition assay (MUH assay). The percentage of growth

inhibition was compared to DMSO-treated controls. Error bars represent SD of three independent experiments. (C and D) Brain melanoma cells were treated with buparlisib for 72 h and then subjected to cell cycle analysis by flow cytometry. Histograms in (C) are representative of triplicate (TueMel32H) or three independent (M10) experiments. The percentage of cells in <G1, G1, S and G2/M phase was quantified and displayed in a stacked bar graph (D). Error bars represent SD.

Figure 4: The PI3K inhibitor buparlisib inhibits AKT activation and induces apoptosis in metastatic melanoma cell lines stimulated with astrocyte-conditioned medium

The WM3734 (BRAF-mutant) metastatic melanoma cell line was cultured in RPMI, astrocyte- (ACM) and fibroblast-conditioned medium (FCM) without FCS and treated with or without 1 μM PI3K inhibitor buparlisib for 30 h. (A) Samples were harvested for Western Blot and analyzed for AKT and pAKT. β-Actin was detected as a loading control. Western Blot is representative of three independent experiments. (B and C) Samples were subjected to cell-cycle analysis by flow cytometry. Histograms in (B) are from three independent experiments. The percentage of cells in <G1, G1, S and G2/M phase was quantified and displayed in a stacked bar graph (C). Error bars represent SD of three independent experiments.

Figure 5: The PI3K inhibitor buparlisib inhibits growth of metastatic melanoma in the brain of nude mice

Representative MRI data of injected WM3734 (BRAF-mutant) human melanoma brain metastasis under buparlisib or sham treatment (A). MRI was performed 16, 20, 23, 27 and 30 days after inoculation. On day 20 post inoculation (p.i.) the treatment was started.

Buparlisib induced stable disease, compared to rapid tumor growth in the sham-treated animals for both BRAF-mutant (WM3734) and NRAS-mutant (SKMel147) brain metastasis, shown by mean values ± SD of the absolute tumor volume (B). For mean value analyses the mice with secure tumor indication at day 19-20 were included (tumor volume ≥ 3 mm^3; n = 8/8 in the BRAF-mutated group; n = 5/5 in the NRAS-mutated group); even if not visible at day 15 in the NRAS-mutated group (n = 3/3 at day 15). Significant differences were reached 7 and 6 days after treatment induction for the BRAF- and NRAS-mutant tumors respectively, as determined by Tuckey-HSD posthoc tests. Kaplan-Meier-plots showed moderate survival for both, the treatment and sham group in BRAF-mutant tumors but dramatically improved survival of the treatment group in NRAS-mutant tumors (C).

Figure 1

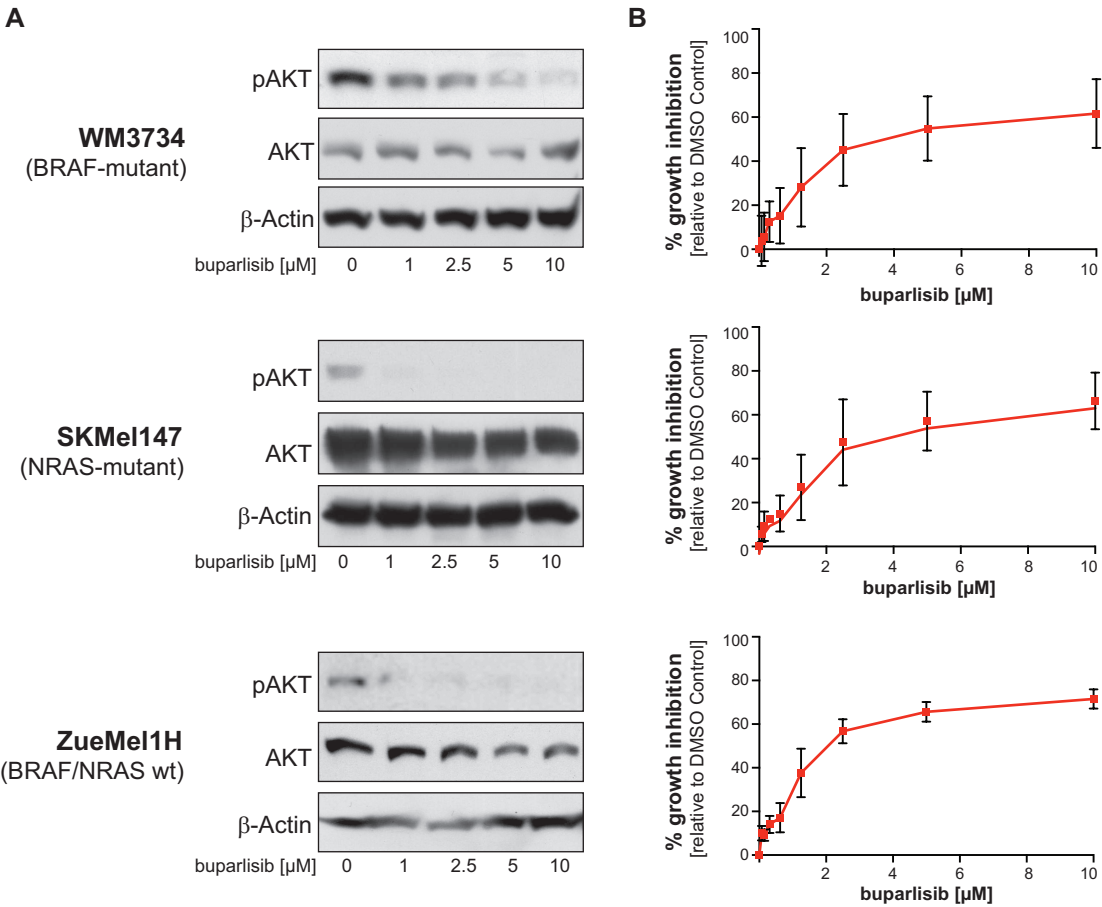
A
B
WM3734
(BRAF-mutant)
SKMel147
(NRAS-mutant)
ZueMel1H
(BRAF/NRAS wt)
pAKT
AKT
β-Actin
buparlisib [μM] 0 1 2.5 5 10
% growth inhibition
[relative to DMSO Control]
buparlisib [μM]

Figure 2

A

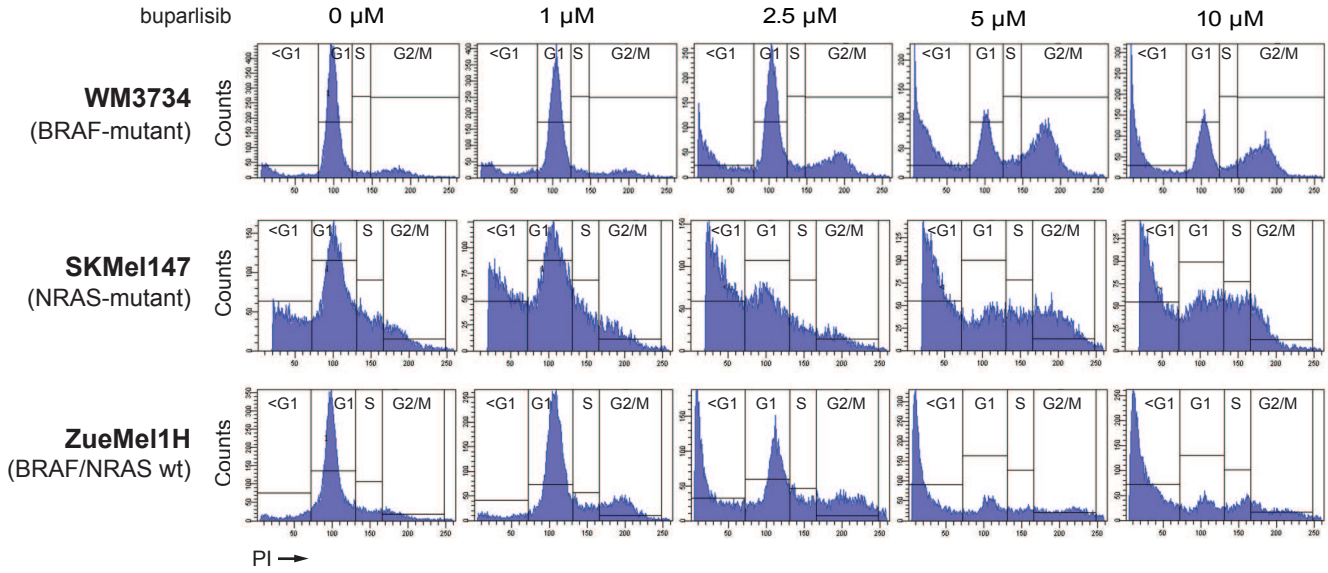
buparlisib
0 µM
1 µM
2.5 µM
5 µM
10 µM
WM3734
(BRAF-mutant)
SKMel147
(NRAS-mutant)
ZueMel1H
(BRAF/NRAS wt)
Counts
<G1
G1
S
G2/M
PI

B

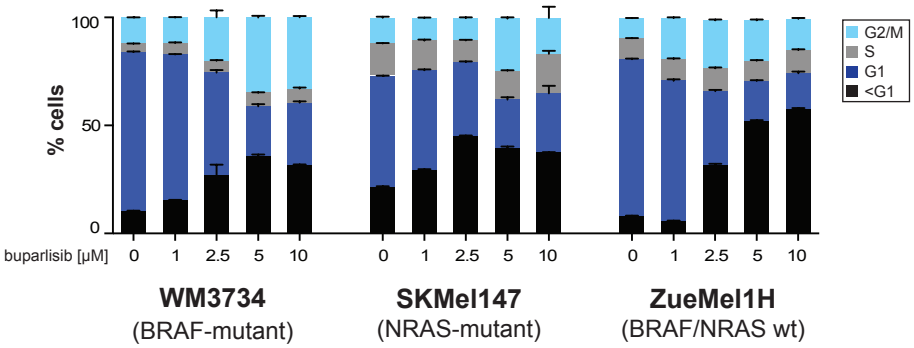
% cells
100
50
0
buparlisib [µM]
0
1
2.5
5
10
G2/M
S
G1
<G1
WM3734
(BRAF-mutant)
SKMel147
(NRAS-mutant)
ZueMel1H
(BRAF/NRAS wt)

Figure 3

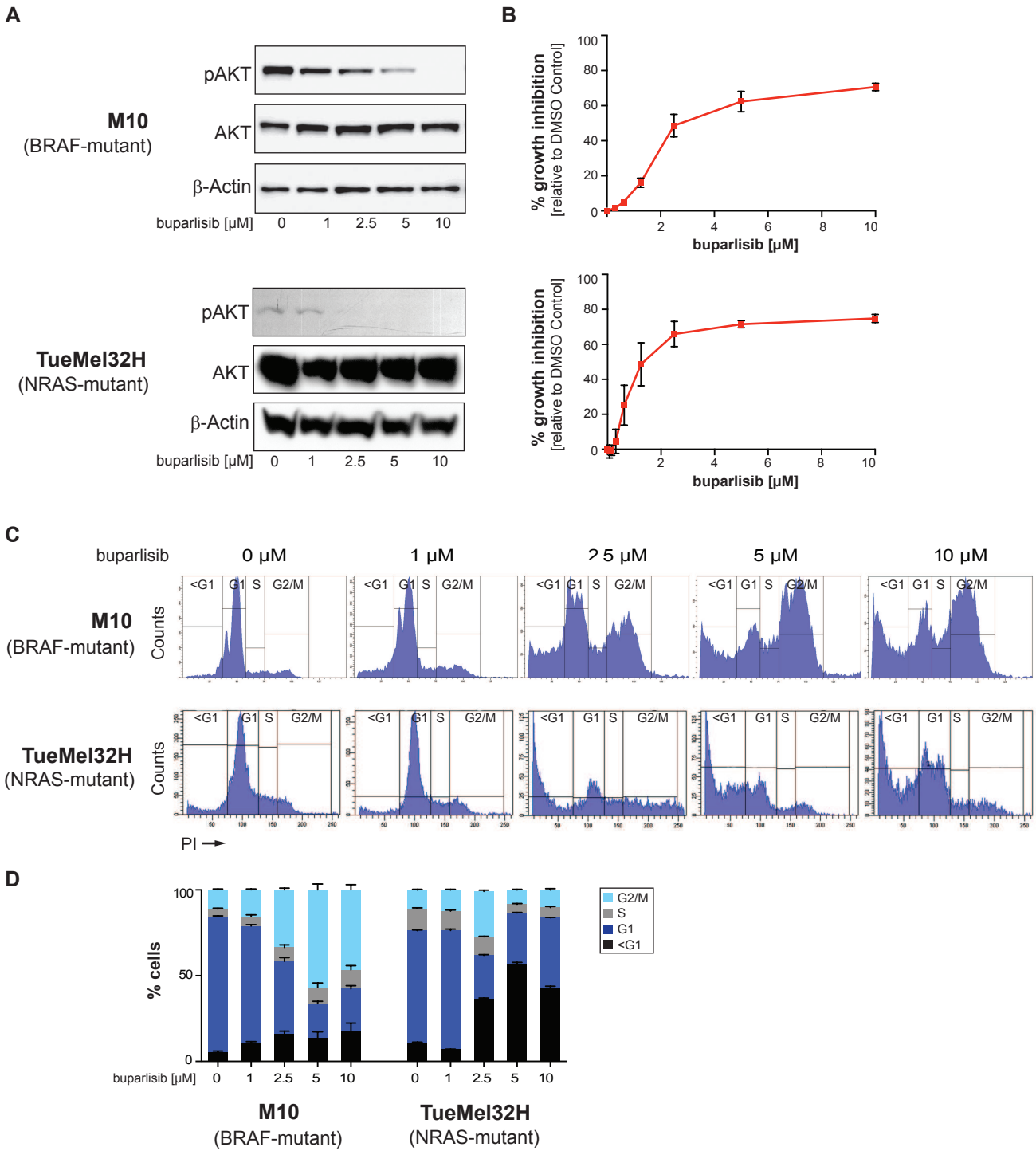
A
M10
(BRAF-mutant)
pAKT
AKT
β-Actin
buparlisib [μM] 0 1 2.5 5 10
TueMel32H
(NRAS-mutant)
pAKT
AKT
β-Actin
buparlisib [μM] 0 1 2.5 5 10
B
% growth inhibition
[relative to DMSO Control]
buparlisib [μM]
% growth inhibition
[relative to DMSO Control]
buparlisib [μM]
C
buparlisib
0 μM
1 μM
2.5 μM
5 μM
10 μM
M10
(BRAF-mutant)
Counts
<G1 G1 S G2/M
TueMel32H
(NRAS-mutant)
Counts
PI
D
% cells
buparlisib [μM] 0 1 2.5 5 10 0 1 2.5 5 10
G2/M
S
G1
<G1
M10
(BRAF-mutant)
TueMel32H
(NRAS-mutant)

Figure 4

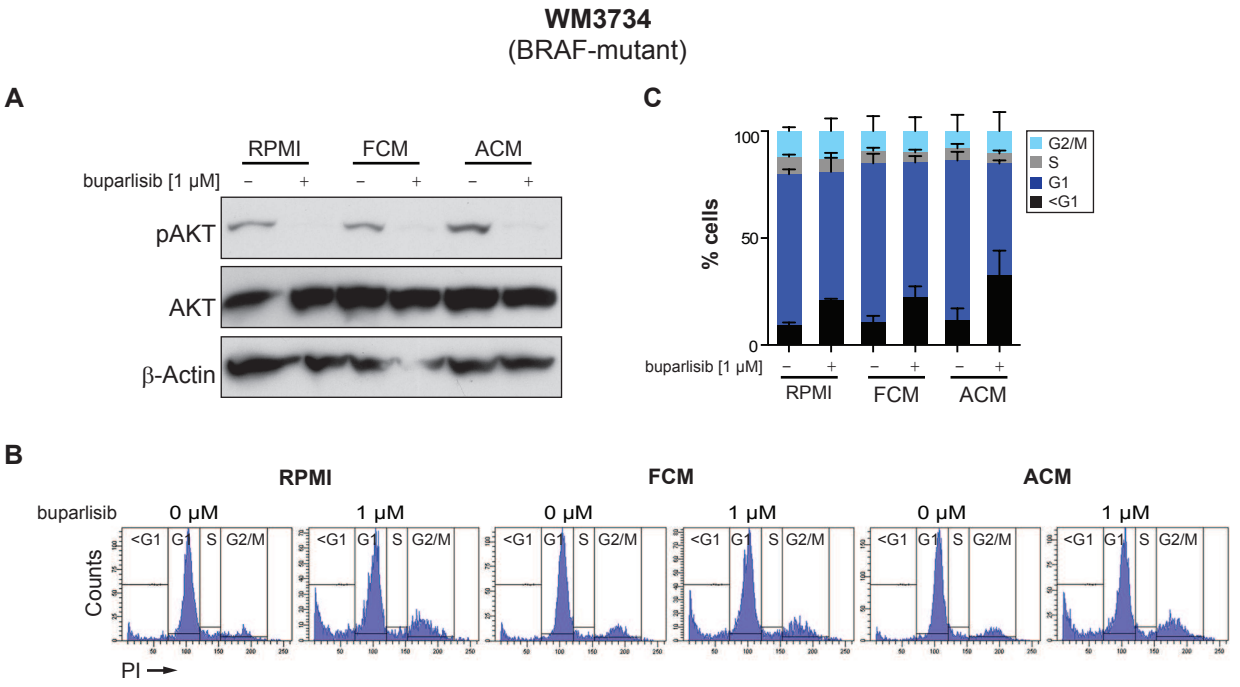
WM3734
(BRAF-mutant)
A
RPMI
FCM
ACM
buparlisib [1 μM]
– + – + – +
pAKT
AKT
β-Actin
C
100
50
0
% cells
G2/M
S
G1
<G1
buparlisib [1 μM]
– + – + – +
RPMI
FCM
ACM
B
RPMI
FCM
ACM
buparlisib
0 μM
1 μM
0 μM
1 μM
0 μM
1 μM
<G1
G1
S
G2/M
Counts
PI

Figure 5

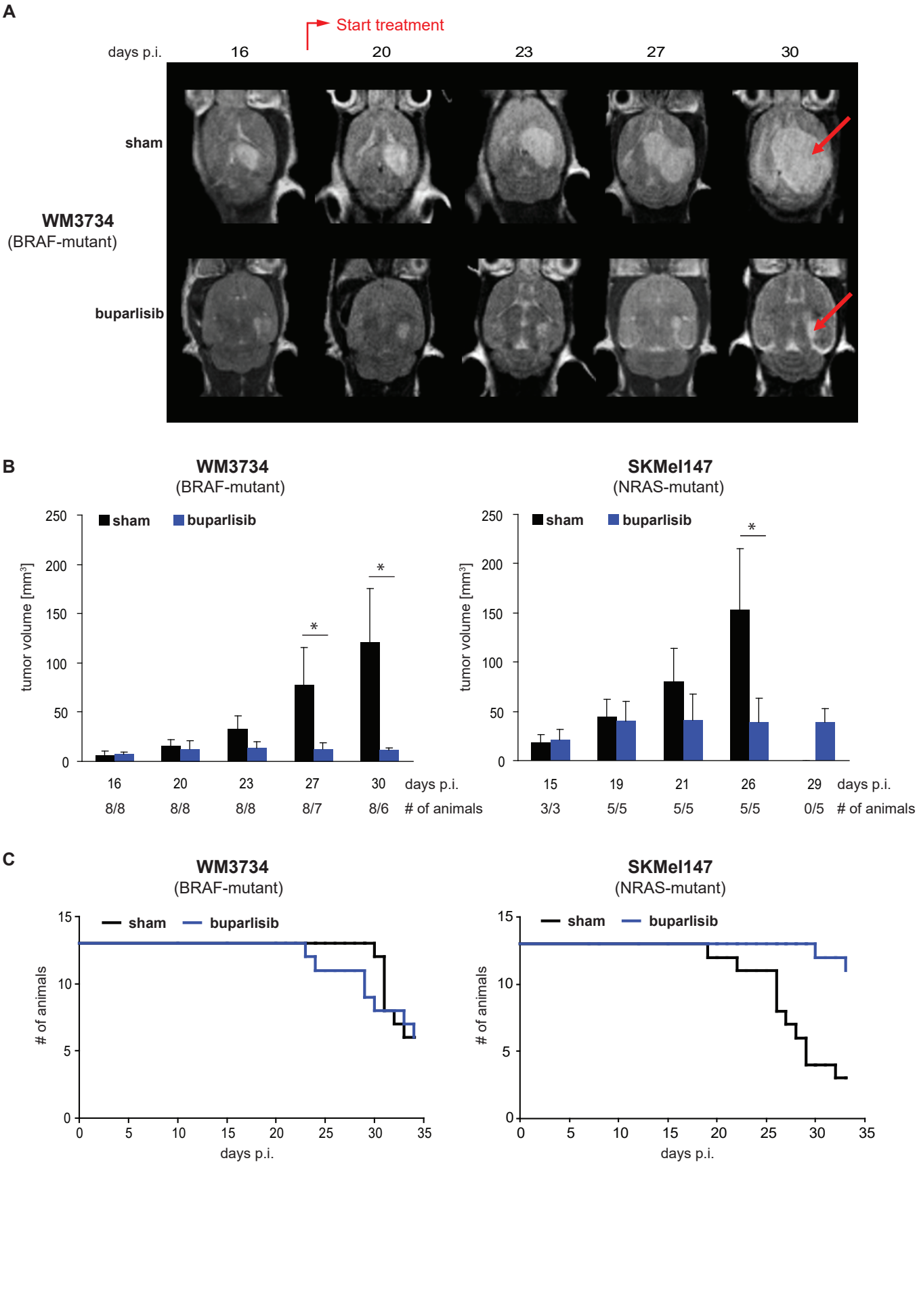
A
Start treatment
days p.i.
16
20
23
27
30
sham
WM3734
(BRAF-mutant)
buparlisib
B
WM3734
(BRAF-mutant)
SKMel147
(NRAS-mutant)
sham
buparlisib
tumor volume [mm³]
250
200
150
100
50
0
*
16
20
23
27
30
days p.i.
8/8
8/8
8/8
8/7
8/6
# of animals
15
19
21
26
29
3/3
5/5
5/5
5/5
0/5
C
WM3734
(BRAF-mutant)
SKMel147
(NRAS-mutant)
sham
buparlisib
# of animals
15
10
5
0
0
5
10
15
20
25
30
35
days p.i.